

Dynamics Simulation of Freight Car Considering the Car Body's Flexible Property

SI FANG ROLLING STOCK RESEARCH INSTITUTE

Cheng hai tao

Abstract: Multi-flex-body dynamics analyzing method is used to simulate the dynamics response of freight car. The studied objects are the open freight C62A car and tank G60 car, whose bogies and wheelsets are thought as flex parts. Finite element model of car bodies are constructed and the modal are analyzed. The flex car bodies are pre-handled by condensing the freedoms of interface through super element concept, the rigid-flex coupling system dynamics equation is constructed and calculated, whose results are compared with those of rigid car bodies system, the effect of elasticity car bodies to the safety of cars are discussed. The effect of elasticity car bodies to the safety of cars are discussed. The simulation is completed by using finite element software NASTRAN(MSC), Mutli-body dynamics software ADAMS/FLEX and ADAMS/Rail.

Key word: freight car, multi-flex-dynamics, FEM, derailment

1. method of constructing flexible car body

1.1 dynamics of flexible car body

define point q to be one point on flexible body, we can get its position in the globe coordinate as the following formula:

$$q = \left\{ \begin{array}{l} x \\ y \\ z \\ \psi \\ \theta \\ \phi \\ p_{j,j=1,m} \end{array} \right\} = \left\{ \begin{array}{l} R \\ \Phi \\ P \end{array} \right\} \quad (1)$$

where: x,y,z defines the position of local reference frame in the global reference frame, ψ, θ, ϕ are the Euler angles of B relative to the global origin, p_j is the modal amplitudes of the m contributing mode shapes, the velocity of the I-th particle can be shown to be:

$$V_i = \left[I - A(\tilde{S}_i + \tilde{\Phi}_i q)B \quad A\Phi_i \right] \dot{q} \quad (2)$$

from which we obtain an expression for the kinetic energy:

$$T = \frac{1}{2} \sum_{i=1}^N m_i V_i^T V_i = \frac{1}{2} \dot{q} M(q) \dot{q} \quad (3)$$

after deriving the mush simpler expressions for the potential energy, we apply lagranges equation to obtain an expression for equations of the flexible body that is used in ADAMS:

$$M\ddot{q} + \dot{M}\dot{q} - \frac{1}{2} \left[\frac{\partial M}{\partial q} \dot{q} \right]^T \dot{q} + Kq + f_g + C\dot{q} + \left[\frac{\partial \psi}{\partial q} \right]^T \lambda = Q \quad (4)$$

equation (4) can be written as: $[M]\{\ddot{q}\} + [C]\{\dot{q}\} + [K]\{q\} = \{F_T\}$

in the equation: K and C denote the modal stiffness and damping matrixes for the flexible body, the damping and stiffness effects are only deformation dependent, therefore, rigid body rotation and

translation do not contribute to strain energy and energy dissipation. f_g denotes the gravitational forces, λ denotes the lagrange multipliers of the constraint, ψ , Q denotes the externally applied load.

1.2 mass matrix of flexible body

M has the following equation:

$$M = \begin{bmatrix} M_{tt} & M_{tr} & M_{tm} \\ & M_{rr} & M_{rm} \\ \text{symmetric} & & M_{mm} \end{bmatrix} \quad (5)$$

The mass matrix in equation 4 is a complicated function of deformation and orientation, but by identifying nine inertia invariants, we greatly improve computational efficiency partitioning the mass matrix into blocks for translational, rotational and modal coordinates we find that:

$$\begin{aligned} M_{tt} &= \sum_{i=1}^N m_i \mathbf{I} = I^1 \mathbf{I} & M_{tr} &= -\sum_{i=1}^N m_i A (\tilde{s}_i + \tilde{\Phi}_i p) \mathbf{B} = -A [I^2 + I_j^3 q_j] \mathbf{B} \\ M_{tm} &= \sum_{i=1}^N m_i A \Phi_i = A I^3 \\ M_{rr} &= \sum_{i=1}^N m_i B^T (\tilde{s}_i + \tilde{\Phi}_i p)^T (\tilde{s}_i + \tilde{\Phi}_i p) \mathbf{B} = B^T [I^7 - [I_j^8 + I_j^{8T}] q_j - I_j^9 q_i q_j] \mathbf{B} \\ M_{rm} &= -\sum_{i=1}^N m_i B^T (\tilde{s}_i + \tilde{\Phi}_i p)^T \Phi_i = B^T [I^4 + I_j^5 q_j] \\ M_{mm} &= \sum_{i=1}^N m_i \Phi_i^T \Phi_i = I^6 \end{aligned}$$

in the mass matrix equation the tilde operator($\tilde{\cdot}$) denotes the skew matrix of a position vector and the matrix B defines the transformation from time derivatives of Euler angles to angular velocity, note that once the invariants I^1 through I^9 have been computed, the dynamics simulation is oblivious to the number of particle comprising the flexible body.

1.3 stiffness matrix of flexible body

the stiffness matrix is constructed by element stiffness matrix because it only concerns with relative deformation, so the matrix can be arrived through constructing virtual power of general elastic force, the virtual power of the I-th element elastic force is as following:

$$\delta W^{ij} = -\int_{V^{ij}} (\sigma^{ij})^T \delta \epsilon^{ij} dV^{ij} \quad (6)$$

in equation (6) σ^{ij} and ϵ^{ij} denote the stress and strain vector, for liner property material in every direction, we have $\sigma^{ij} = E^{ij} \epsilon^{ij}$ in the equation E^{ij} denotes the modulus of elasticity matrix. The relation between stress and strain is as the following:

$$\epsilon^{ij} = D^{ij} u_f^i \quad (7)$$

where D^{ij} denotes the deviating differential operator.

We have the following equation:

$$u_f^i = N^{ij} q_f^i \quad (8)$$

where N^{ij}, q_f^i denote the form function of the I-th element in body coordinate system and the displacement vector of the I-th node. So we have the following function:

$$\epsilon^{ij} = D^{ij} N^{ij} q_f^i \quad (9)$$

replace the $\varepsilon^{ij}, \sigma^{ij}$ in equation (6) with function (7)~(9), we have the following expression:

$$\delta W^{ij} = -\left(q_f^i\right)^T K_{ff}^{ii} \delta q_f^i \quad (10)$$

where K_{ff}^{ii} denotes the stiffness matrix of element I, after assembling the stiffness matrix of element we can get the stiffness matrix of body as the following:

$$K_{ff} = \sum_{j=1}^{n_e} K_{ff}^{ii} \quad (11)$$

1.4 damping matrix of the flexible body

the damping matrix in equation (4) can be arrived by summing each row element value of well-distributed damping matrix as the diagonal line element value, and set the value of non-diagonal line to be zero, the damping matrix of well-distributed is as the following equation:

$$C = (c_{kl})_{l_i \times l_j}, \quad c_{kl} = \int_{\Omega_i} \phi_{ik} \phi_{il} dx$$

considering $\sum_{i=1}^{l_i} \phi_{il} = 1$ so the concentrating damping matrix is as the following:

$$C = \text{diag}(c_i) \quad c_i = \int_{\Omega_i} \phi_i dx$$

2. FEM modal and mode analysis result

2.1 FEM modal

The FEM modals are based on the C62A open car body and the G60 tank car body which are the most popular used two types freight cars in the People's Republic of China, according to the structure of the freight car body we construct the FEM modal, the FEM modal is constructed and analyzed by using the NASTRAN(MSC) software. For open wagon there are 10347 nodes and 10930 elements, for tank wagon, the shape is relative simple, so the nodes and element of its are more scattered, there are 414 nodes and 430 elements. The shapes of the element are triangle and quadrilateral. All the element are plate elements, the thickness of which varies with the thickness of real structures.

2.2 results of mode analysis

there are 32 modes in the analyses results, the first 6 modes are rigid body modes, during dynamics analyzing the rigid body modes are omitted. Table 1 shows the first 7-12 modes of open wagon car body and tank wagon car body, from the frequency we can see that the frequency of tank wagon car body is higher than that of open wagon car body, this is consistent with realistic condition.

Table 1 the first 7~12 modes of C62A open wagon car body

mode	Car body type	Mode type	C62A car body(Hz)	Tank wagon car body(Hz)
7		First rolling	1.101	10.178
8		First twisting	4.061	20.637
9		First vertical bending	17.525	23.923
10		First lateral bending	20.644	26.739
11		Second lateral bending	22.139	28.572
12		Second vertical bending	22.296	32.039

Figure 1 through 4 show the deforming mode of C62A open wagon car body.

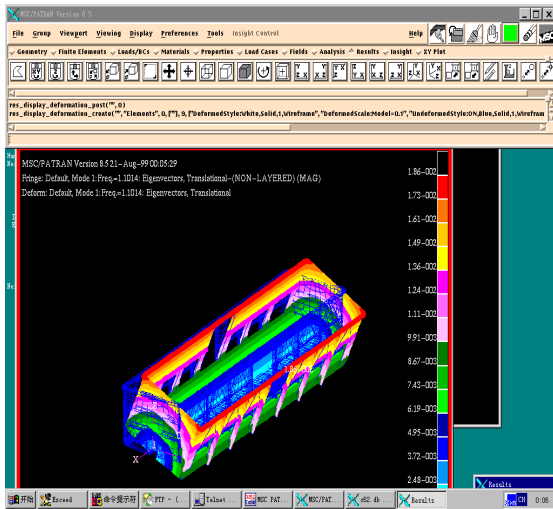


Figure1 first mode of C62A open wagon car body

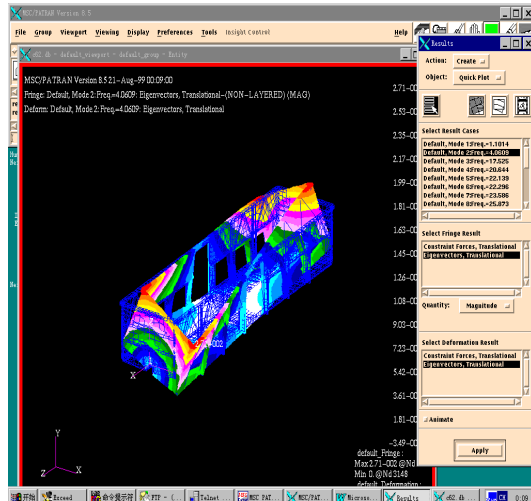


Figure2 second mode of C62A open wagon car body

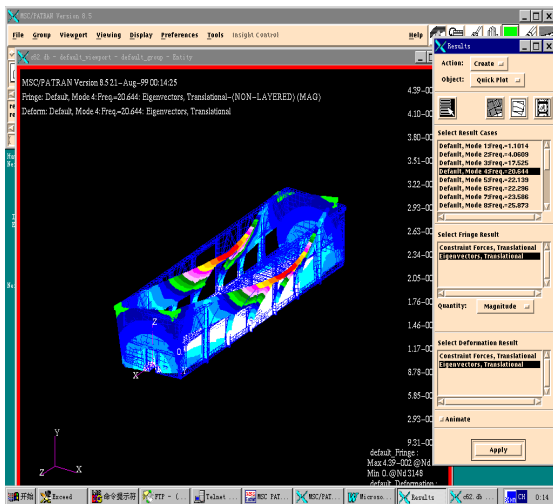


Figure3 third mode of C62A open wagon car body

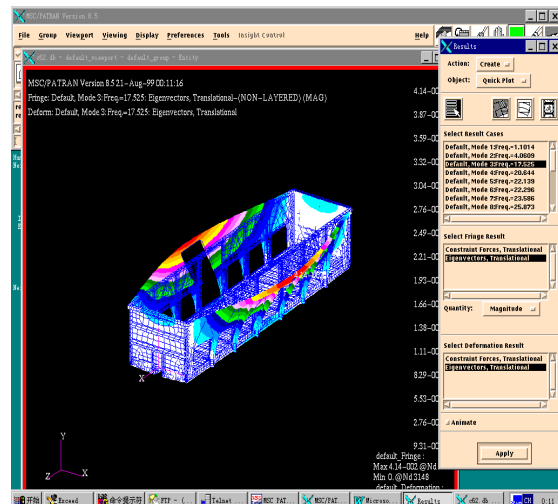


Figure4 fourth mode of C62A open wagon car body

3 contrast and analyzing of rigid and rigid-flex coupling system calculation result

After importing the FEM modal into ADAMS/Rail, figure 5 and 6 show the dynamics system analysis model of open wagon and tank wagon. figure 7 and 8 show the rigid car body system modal.

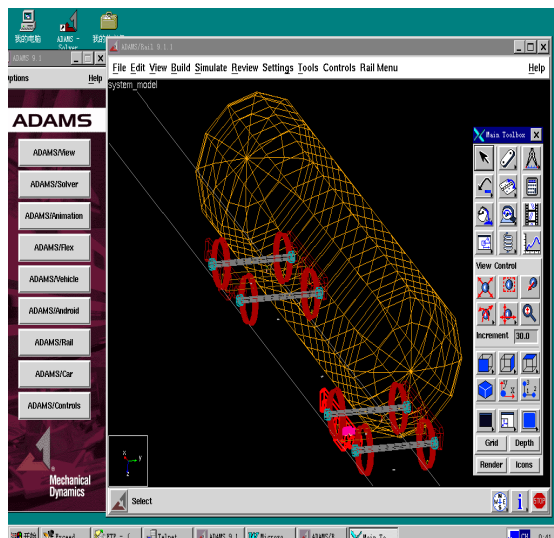
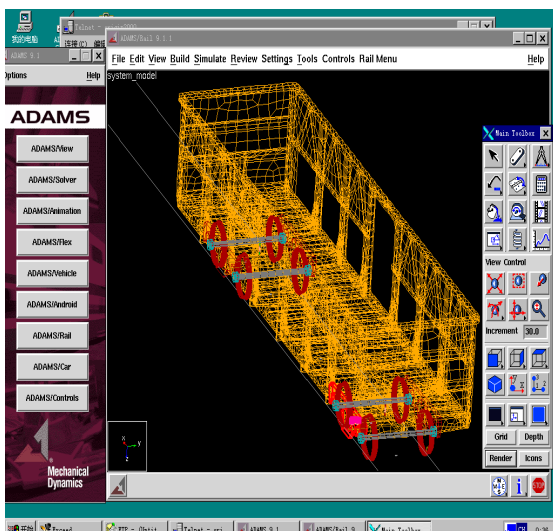


Figure 5 rigid-flexible coupling system modal of C62A

Figure 6 rigid-flexible coupling system modal of G60

Figure 7 rigid system modal of C62A

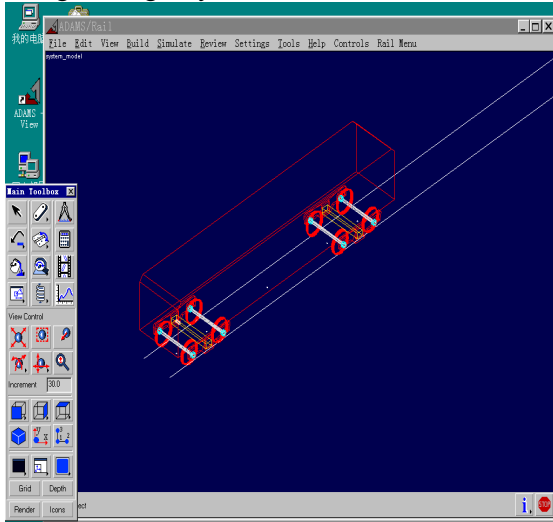
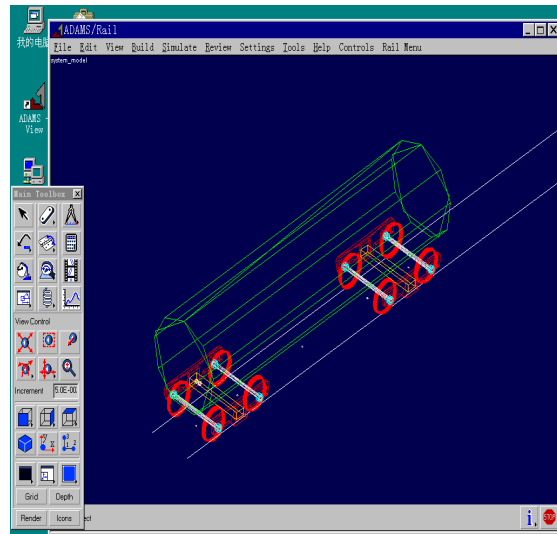


Figure 8 rigid system modal of G60



Calculating the system built above respectively, during the calculation, using AAR psd5 as the line disturbance. To avoid calculation difficulty, there is a distance which has no disturbance. The speed is 80km/h. figure 9~14 are the result contrast between rigid system and rigid-flex system.

contrast of wheelsets 1 lateral/vertical force Ratio between rigid-flex coupling system and rigid system

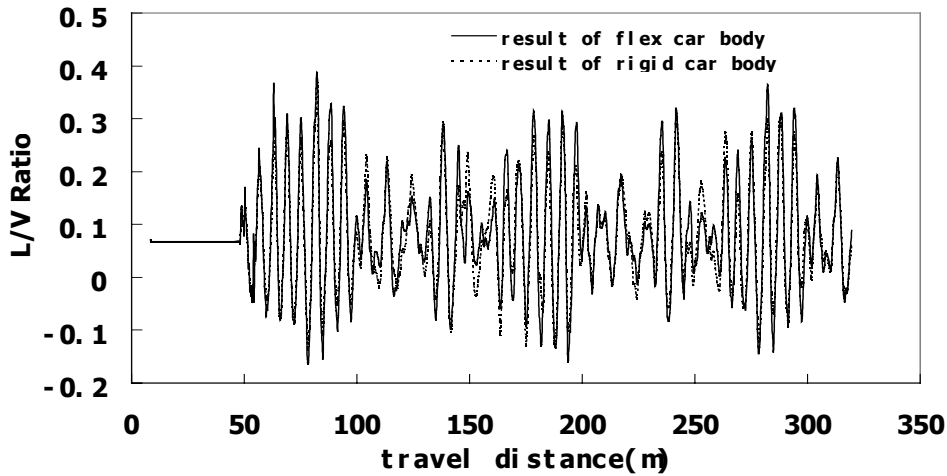


Figure 9 L/V Ratio contrast of C62A flex car body and rigid car body

contrast of wheelsets 1 vertical/force decreasing Ratio between rigid-flex coupling system and rigid system

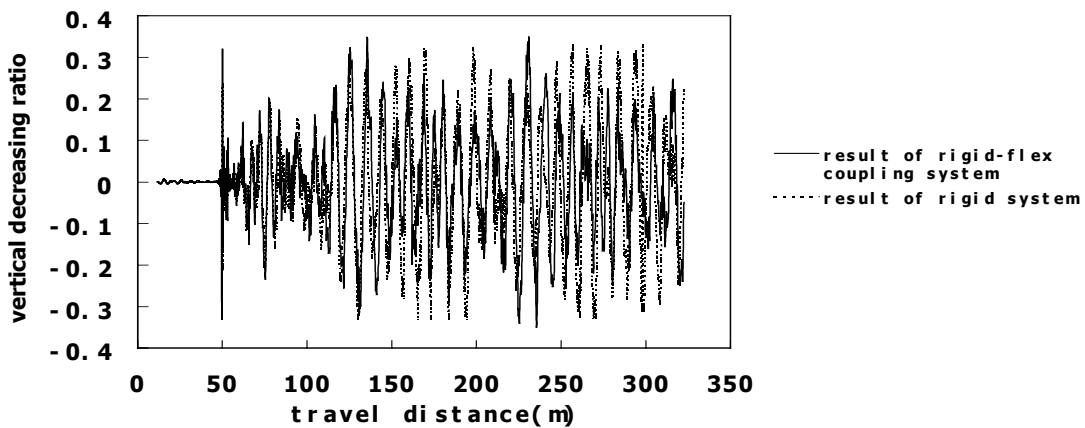


Figure 10 vertical force decreasing Ratio contrast of C62A flex car body and rigid car body

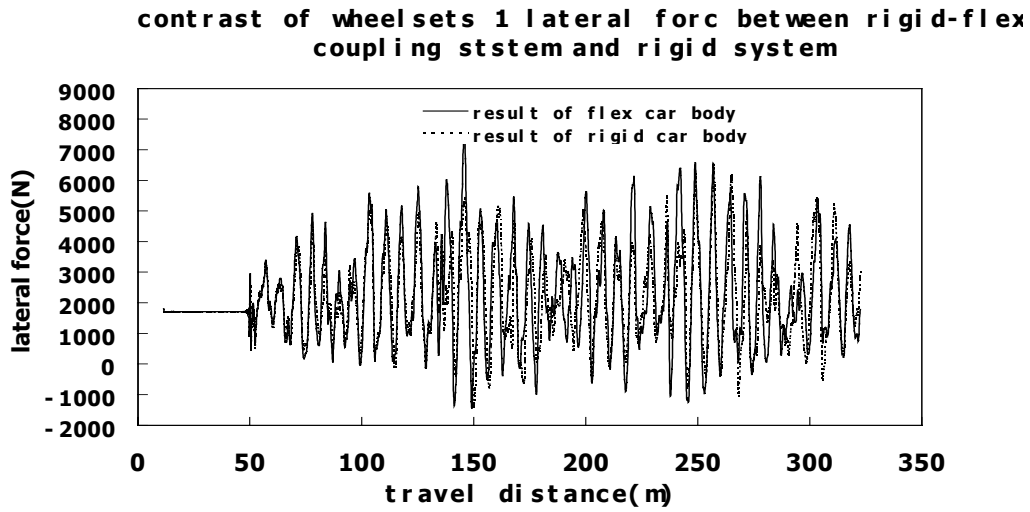


Figure 11 lateral force contrast of C62A flex car body and rigid car body

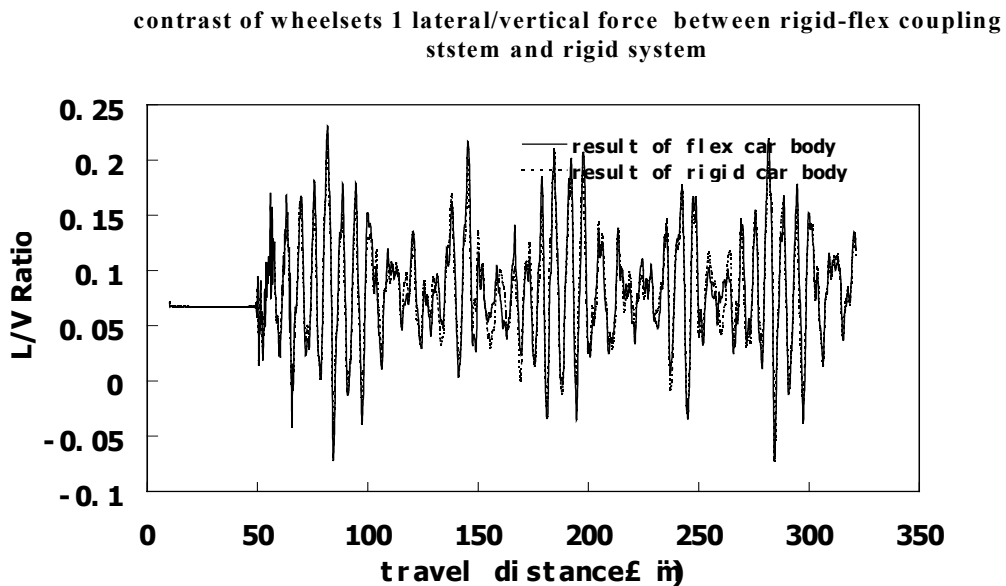


Figure 12 lateral/vertical force ratio contrast of G60 flex car body and rigid car body

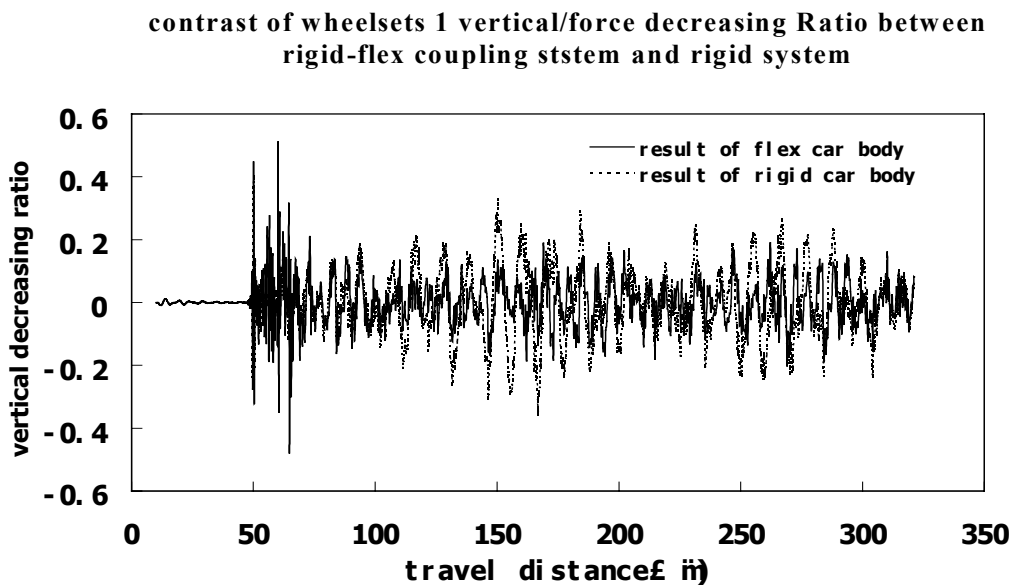


Figure 13 vertical force decreasing ratio contrast of G60 flex car body and rigid car body

contrast of wheelsets 1 lateral displacement between rigid-flex coupling system and rigid system

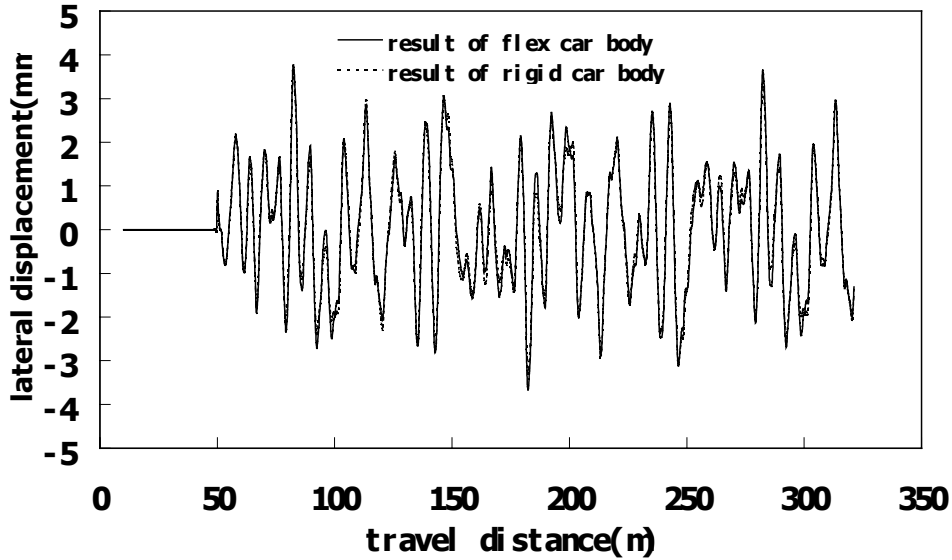


figure 14 lateral displacement contrast of G60 flex car body and rigid car body

From the contrast of lateral displacement, lateral force, lateral/vertical force ratio we can see that when there is no line disturbance the result of flex-rigid and rigid modal are almost the same. When adding the line disturbance, the max value of lateral/vertical force ratio and lateral force are larger than that of rigid car modal. From figure 10 and figure 13 we can see that the vertical force ratio is smaller than that of rigid modal, and the curve changes more smoothly than that of rigid modal, the vertical force ratio changes violently between two max values. From figure 14 we can see that the lateral displacement of wheelsets is of little difference between two modal.

4. summary

To handle some parts of railway vehicle as flex bodies and to assemble the flex bodies with other rigid parts forming a rigid-flex coupling dynamics system analyzing modal is the direction of dynamics analysis in the future. The writer does some complete research work in this article. In the same disturbance line and the same running speed, the max value of lateral/vertical force ratio and lateral force of wheelsets of flex car body are bigger than that of rigid car body, but during the transition period between two max value, the result of flex car body is more smoothly than that of rigid car body, the vertical force ratio is smaller than that of rigid modal, the lateral displacement of wheelsets is of little difference between two modal.